MONITORING SEA ICE USING ENVISAT ASAR – A NEW ERA STARTING 10 YEARS AGO

Wolfgang Dierking[1] *and Leif Toudal Pedersen*[2]

[1]Alfred Wegener Institute for Polar and Marine Research, Wolfgang.Dierking@awi.de
[2]Danish Meteorological Institute, ltp@dmi.dk

ABSTRACT

A short overview is given on the achievements made in sea ice monitoring during the last decade utilizing the technical possibilities of Envisat ASAR. In particular we discuss the improvements by employing the dual-polarization image mode, the benefits of the wide-swath capability, and the advantage to select between seven swaths at different incidence angle ranges when using the image mode.

Index Terms— Envisat, SAR, sea ice monitoring

1. INTRODUCTION

Space-borne synthetic aperture radar (SAR) can be operated independent of daylight and cloud conditions and provides images with comparatively high spatial resolutions on the order of 10 meters or even better. SAR imagery is used to support operational sea ice mapping, to provide data on sea ice conditions for scientific studies on atmosphere / sea ice / ocean interactions, to improve and extend theoretical models for simulating radar scattering from sea ice, and to develop methods for retrieval of sea ice parameters. For operational sea ice mapping, SAR images need to be available in near real time on a daily basis [10]. Both for operational and scientific purposes information is required on the position of the ice edge, on ice concentration (fraction of ice in a given area), ice type distribution, ice thickness and ice drift [11]. In environmental monitoring and climate research, SAR images are also used, e.g., to determine the timing of melt-onset and freeze-up in the Polar Regions, and for retrieval of melt pond coverage on the ice.

2. TECHNICAL IMPROVEMENTS OFFERED BY ENVISAT ASAR

Before ENIVSAT Advanced SAR (ASAR) data became available in 2002, C-band SAR images from ERS-1 (1990-2000), ERS-2 (1995-2011), and Radarsat (launched in 1995) have been used for sea ice observations. These SAR instruments were one-channel systems. The ERS-1/2 SARs were operated at VV-polarization and provided images of 100 km width across-track, covering an incidence angle range from 19.4-26.4°, with a spatial resolution of 30 m. The nominal ERS1/2 repeat cycle was 35 days. Radarsat is still in operation. It measures data at HH-polarization, the repeat cycle is 24 days. A number of imaging ("beam") modes can be selected that differ in swath width (50-500 km), spatial resolution (8-100 m), and incidence angle range (selectable in the interval 10-59°).

Also the ENVISAT ASAR provided different imaging geometries: swath widths from 56 to 400 km, spatial resolutions from 30 m to 1 km, and a total incidence angle range from 15 to 45°. Data acquisitions could be carried out at VV- or HH-polarization. In the alternating-polarization (AP) or dual-polarization mode, two interleaving images were acquired, either at VV/HH, VV/VH or HH/HV. The noise level of the AP-mode varied between -19 dB and -27 dB, dependent on swath and incidence angle. For sea ice monitoring, it was of large interest to investigate potential gains of the dual-polarization capability, the wide-swath mode with 400 km extension across-track, and the choice of different incidence angle intervals for imaging modes with a narrow swath. Corresponding results are described in the following sections. A list of selected relevant publications is provided, which include further important references. Many of the results reported here are valid only under freezing conditions but not for the melt season during which the radar signal does not penetrate a wet snow layer or a wet ice surface.

3. SENSITIVITY TO POLARIZATION AND INCIDENCE ANGL

Like-polarization VV and HH: At HH-polarization, the backscattering coefficient σ^0_{HH} of smoother surfaces decreases faster as a function of incidence angle than at VV-polarization. Hence, the contrast between smooth level ice and rough ice is larger at HH-polarization and increases with incidence angle [1]. For ice-water discrimination, HH-polarization is better suited since ocean clutter is more suppressed than at VV-polarization [9] (the effect of the wind has to be considered nonetheless: a water surface generally appears brighter in SAR images at higher wind speed). For operational sea ice mapping, HH-polarization is preferred.

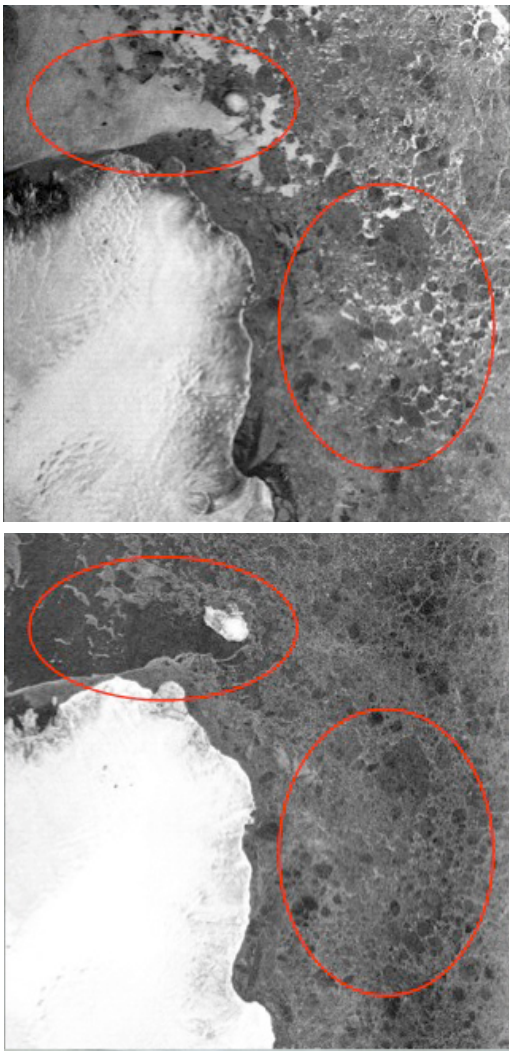

Figure 1. ASAR dual-polarization images acquired over sea ice northeast of Nordaustlandet/Svalbard, on March 17, 2007. Top: HH-, bottom: HV-polarization. The swath width is 100 km, the incidence angle range 15°-22.9°. Near range is to the right. Wind speed was 10 m/s, therefore large open water areas appear bright at HH-polarization (ellipse top left) but also smaller water patches between ice floes can be recognized (ellipse bottom right). (Copyright: ESA)

Cross-polarization HV and VH: The cross-polarized radar backscattering is not sensitive to the incidence angle and is less sensitive to wind speed [9]. A water surface appears mainly dark (see Fig. 1). Therefore, icebergs in the open ocean are more easily recognized in cross-polarized SAR images. Since depolarization is stronger for rougher thin ice than for water, the former can be better separated from the latter than at like-polarization. Large-scale roughness features on the ice surface and ice volume inhomogeneities influence the backscattered cross-polarized signal [14]. Hence, separation between multi-year and first-year ice and between level and deformed ice is easier [9]. For Baltic sea ice, C-band VH-polarization at larger incidence angles (about 45°) was found to be optimal for ice type classification [6]. A general problem of recent satellite SAR systems is the low signal-to-noise ratio of the cross-polarization channels.

Incidence angle θ: Multi-year ice is characterized by a low-salinity and a high volume fraction of air bubbles. The salinity of first-year is higher, and it usually contains less air bubbles. Hence, the radar response from first-year is dominated by surface scattering. In the case of multi-year ice, also volume scattering from the air bubbles has to be considered. The radar intensity arising from surface scattering decreases faster as a function of θ than from volume scattering (for $20°<\theta<55°$). Multi- and first-year ice can therefore better be distinguished at larger values of θ [1]. In some cases, also ridges are easier to identify at larger incidence angles [1]. These examples show that the option of different swaths for image (IM-) mode data acquisitions (i. e. different incidence angle ranges) is advantageous. It also includes the possibilities to combine images of a given area acquired at different incidence angles, and, by doing so, to decrease the time interval between single data takes if required.

4. USE OF DUAL-POLARIZATION MODE FOR ICE TYPE CLASSIFICATION

Co-polarization ratio: Dependent on surface characteristics, the co-polarization ratio $\gamma_{VV/HH}$ increases more or less strongly at larger incidence angles. For incidence angles >35°, it is useful for discrimination of rough first-year and multi-year ice ($\gamma_{VV/HH}$ of about 0 dB) and open water ($\gamma_{VV/HH}$ > 0 dB), considering the fact that it is only slightly sensitive to wind speed [9] [4]. Also new and young ice with smooth surfaces reveal a $\gamma_{VV/HH} > 0$ dB [4]. The difference between VV- and HH-polarization is less sensitive to small-scale surface roughness than to the dielectric constant of the ice surface, which is, in turn, related to ice thickness via corresponding changes in the near-surface ice salinity. In one study, ice thickness (for ice up to about 1.2 m thick) could be retrieved with a sufficient accuracy based on the co-polarization ratio at C-band [8]. In general, however, ice thickness is difficult to retrieve from SAR images. Under summer conditions it was found that $\gamma_{VV/HH}$ is correlated with the optical surface albedo when the ice surface is covered by unfrozen melt ponds. The wind generates small ripple waves on the pond surface, which leads to a backscattering characteristic of slightly rough surfaces. The larger the fraction of ponds, the larger is $\gamma_{VV/HH}$ and the lower the albedo [13].

Cross-polarization ratio: Because of the relatively high noise level of ENVISAT ASAR, cross-polarization ratios HH/HV and VV/VH are more useful at smaller incidence angles (< 30°) for discriminating water, slush/grease ice, consolidated pancake ice, and multi-year ice. Other ice types

cannot be separated using dual-polarization HH/HV and VV/VH. This is due to the combined effects of frost flowers, snow, and ice deformation in particular for nilas, grey ice and thin first-year ice [9]. The Canadian Ice Service (CIS) has identified the following areas for which combinations of HH and HV aid an ice-analyst: detection of multi-year ice embedded in first-year ice, ice vs. open water separation, detection of leads, and ice concentration estimates [13].

5. SWATH WIDTH AND SPATIAL RESOLUTION

The advantage of the wide swath (WS) mode (also called ScanSAR-mode in the case of Radarsat) is the large spatial and good temporal coverage of sea ice areas in the Polar Regions [11]. For example, over Svalbard images can be obtained twice a day from the descending (morning pass) and ascending (evening pass) orbit. This means that also short-term (less than 12 hours) changes of the ice cover (drift, deformation) can be studied. Because of the sensitivity of the backscattering coefficient σ^0 to the radar incidence angle θ and the large incidence angle range covered by ASAR WSM, correction schemes have to be applied. This is not a trivial task since the sensitivity of σ^0 to θ depends on the surface type and is stronger for smoother surfaces (new level ice, calm water) than for rougher ones (deformed ice, wind-roughened water) for $20°<\theta<55°$. It is also larger for wet snow than for dry snow [5]. Due to the rapid temporal change of the sea ice cover, operational charting almost entirely relies on the wide-swath mode, which provides the most frequent coverage.

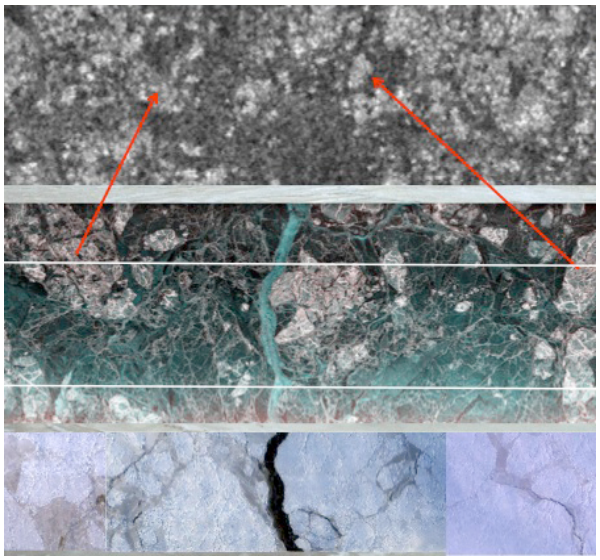

Figure 2. Images acquired over Fram Strait on March 19, 2007. Top: Zoom-in of ASAR wide-swath image, HH-pol., local incidence angle 26°, middle: airborne C-band SAR (ESAR; RGB with R=VH, G=VV, B=VV), bottom: optical scanner. The width of the radar strips is 3 km, the position of the optical strip is indicated in the ESAR image. Acquisition times: ASAR 1122UTC, ESA 12:26UTC

One disadvantage is, at least in some cases, the coarse spatial resolution of 150 m at WS-mode, which, on the other hand, is partly compensated by a higher number of looks (=12). For the AP-mode, the corresponding numbers are 30 m and 2. To reduce speckle (which causes a grainy appearance of the original AP-images) and increase the number of looks, adjacent pixels have to be averaged at the cost of decreasing the resolution. Even smaller ice features can be well recognized in WS-imagery if their intensity contrast relative to their neighborhood is large, as Fig. 2 demonstrates. Here, thicker and older ice floes with rougher surfaces are embedded in new thin ice with a smooth surface. The lead visible in the middle of the airborne SAR image, however, cannot be identified in the WS-image.

6. ENVIRONMENTAL EFFECTS

The influence of wind speed on the separation of open water and sea ice was already discussed above. The wind direction relative to the radar look direction is another factor that determines the radar intensity backscattered from open water areas. Problems in classifying such areas correctly can be alleviated by combining images acquired at dual-polarization mode. Another important environmental parameter influencing sea ice classification is the air temperature. Under melting conditions, the penetration depth of C-band radar waves is reduced to a few millimeters to centimeters, and the measured intensity is entirely dominated by surface contributions. Older ice, under freezing conditions with a large contribution of volume scattering, reveals lower radar intensities if the snow cover or the ice surface is wet (see Fig. 3). Also surface roughness may decrease under melting conditions. The onset of melting complicates operational sea ice mapping. However, the radar signature changes related to melt-onset and freeze-up are used to determine their dates and the duration of the melt season. This information is valuable for investigations focusing on climate change in the Polar Regions [15], [16].

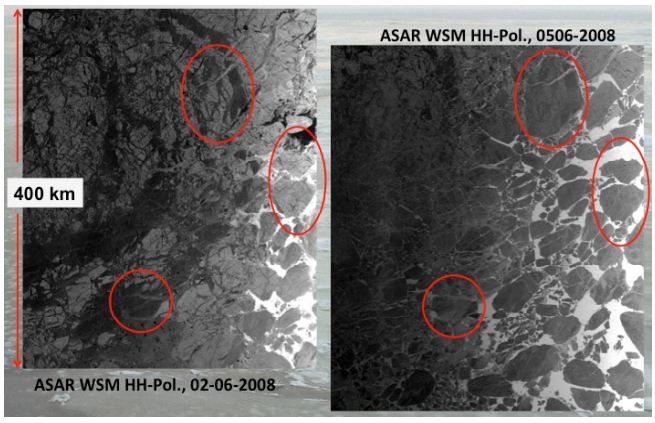

Figure 3. ASAR wide-swath mode images acquired over the Beaufort Sea on June 2 and June 5, 2008, showing the effect of melt-onset.

7. COMPARISON WITH OTHER FREQUENCY BANDS (X- AND L-BAND)

The signature contrast between deformation zones (ridges, rubble fields, brash ice) and smooth level ice is larger at L-band than at higher radar frequencies [1] [5]. Because of the larger penetration depth of longer radar waves, L-band is superior for sea ice mapping during the melting period compared to C- and X-band [1]. For a reliable detection of melt onset and freeze-up, higher radar frequencies are preferable [1]. In a number of investigated cases it was found that the total ice type classification accuracy (adding the errors for all ice types in a scene) was better at L-band than at C-band [1]. In single cases, however, C-band radar performs better, e. g. for sea ice regimes without significant occurrence of deformation features such as ridges, rubble fields, or brash ice. Higher-frequency radars are more sensitive to the small-scale surface roughness and volume inhomogeneities, which means that they in general are better suited for discrimination of different stages of new ice. However, studies revealed that L-band can provide better classification accuracies in certain cases [2]. For retrieving the thickness of undeformed first-year ice, L-band is better suited than C-band since the co-polarization ratio is almost independent of surface roughness for the former [7]. The information content on sea ice properties is largely equivalent at X- and C-band [3] but reveals some differences in the correlation and phase differences between the HH- and VV-channel [2].

8. CONCLUSIONS

The Envisat era is characterized by many valuable improvements to sea ice monitoring and research, either by making use of the ASAR images for interpretation, analyses, and parameter retrievals, or by studying the potential of different imaging modes in conjunction with other satellite missions, airborne measurements, and/or field data acquisitions. Studies on Envisat ASAR data contributed significantly to increase the utilization of radar imagery for operational and environmental applications, which is reflected in a number of projects such as MyOcean (www.myocean.eu) or PolarView (www.seaice.dk), both contributing to the European "Global Montoring for Environment and Security GMES" program (www.gmes.info).

9. REFERENCES

[1] Dierking, W., T. Busche, Sea ice monitoring by L-band SAR: An assessement based on literature and comparisons of JERS-1 and ERS-1 imagery, *IEEE Trans. Geosci: Rem. Sens.*, Vol 44, No. 2, pp. 957-979, 2006

[2] Dierking, W., Thin ice classification and thickness estimation using ASAR, PALSAR, Radarsat-2 and TerraSAR-X data: First results, *Proceedings of ESA Living Planet Symposium 2010,* Bergen, Norway, ESA SP-686 (on CD-ROM), 2010

[3] Eriksson, L. E. B., Borenäs, K., Dierking, W., Berg, A., Santoro, M., Pemberton, P., Lindh, H., Karlson, B, Evaluation of new spaceborne SAR sensors for sea-ice monitoring in the Baltic Sea, *Canadian Journal of Remote Sensing*, Vol. 36, Suppl. 1, pp. S56-S73, 2010

[4] Geldsetzer, T., and J. J. Yackel, Sea ice type and open water discrimination using dual co-polarized C-band SAR, *Can. J. Remote Sensing*, Vol. 35, No. 1, pp. 73-84, 2009

[5] Mäkynen, M. P., A. T. Manninen, M. H. Similä, J. A. Karvonen, and M. T. Hallikainen, Incidence angle dependence of the statistical properties of C-band HH-polarization backscattering signatures of the Baltic Sea ice, *IEEE Trans. Geosci. Rem. Sens.,* Vol 40, No. 12, pp. 2593-2605, 2002

[6] Mäkynen, M., and M. Hallikainen, Investigations of C- and X-band backscattering signatures of Baltic Sea ice, *Int. J. Remote Sensing*, Vol. 25, No. 11, pp. 2061-2086, 2004

[7] Nakamura, K., H. Wakabayashi, S. Uto, K. Naoik, F. Nishio, and S. Uratsuka, Sea ice thickness retrieval in the Sea of Okhotsk using dual-polarization data, *Annals of Glaciology* 44, pp.261-268, 2006

[8] Nakamura, K., H. Wakabayashi, S. Uto, S. Ushio, and F. Nishio. Observation of sea ice thickness using ENVISAT data from Lützow-Holm Bay, East-Antarctica, *IEEE Geosc. Rem. Sens. Letters*, Vol. 6, No. 2, pp. 277-281, 2009

[9] Partington, K. C., J. D. Flach, D. Barber, D. Isleifson, P. J. Meadows, and P. Verlaan, Dual-polarization C-band radar observations of sea ice in the Amundsen Gulf, *IEEE Trans. Geosc. Rem. Sens.*, Vol. 48, No. 6, pp. 2685-2691, 2010

[10] Pedersen, L.T. and R. Saldo, Experience with near real time distribution of Envisat ASAR data to end-users. In Lacoste, H. and L. Ouwehand, eds. Proceedings of the 2004 Envisat and ERS symposium, ESA Publications Division. (ESA SP-752.) CD-ROM, 2005

[11] Sandven, S., K. Kloster, H. Tangen, T. S. Andreassen, H. Goodwin, and K. Partington, Sea ice mapping using Envisat ASAR wideswath images, *Proc. 2nd Workshop Coastal and Marine Applications of SAR*, ESA SP-565, June 2004

[12] Scharien, R. K,, J. J. Yackel, M. A. Granskog, and B. G. T. Else, Coincident high resolution optical-SAR image analysis for surface albedo estimation of first-year sea ice during summer melt, *Remote Sensing of Environment* 111, pp. 160-171, 2007

[13] Scheuchl, B., R. Caves, D. Flett, R. DeAbreu, M.Arkett, and I. G. Cumming. The potential of cross-polarization information for operational sea ice monitoring, *Proc. ENVISAT/ERS Symposium*, Salzburg, Austria, September 6-10, 2004

[14] Scheuchl, B., D. Flett, R. Caves, and I. Cumming, Potential of Radarsat-2 data for operational sea ice monitoring, *Can. J. Remote Sensing*, Vol. 30, No. 3, pp. 448-461, 2004

[15] D. P.Winebrenner, E. D. Nelson, R. Colony, and R. D.West, Observation of melt onset on multiyear arctic sea ice using the ERS-1 synthetic aperture radar, *J. Geophys. Res.*, Vol. 99, No. C11, pp. 22 425–22 441, 1994

[16] D. P. Winebrenner, B. Holt, and E. D. Nelson, Observation of autumn freeze-up in the Beaufort and Chukchi Seas using the ERS-1 synthetic aperture radar, J. Geophys. Res., vol. 101, no. C7, pp. 16 401–16419, 1996